Genes, Brain and Behavior
Official publication of the International Behavioural and Neural Genetics Society

Genes, Brain and Behavior (2016) ***15:*** *335–347* doi: 10.1111/gbb.12281

Scn1a dysfunction alters behavior but not the effect of stress on seizure response

N. T. Sawyer[†,‡,1,*], A. W. Helvig[§,1], C. D. Makinson[†], M. J. Decker[¶,], G. N. Neigh[††,‡‡] and A. Escayg[†]**

[†]Department of Human Genetics, Emory University, Atlanta, GA, [‡]Department of Biology, Clayton State University, Morrow, GA, [§]Byrdine F. Lewis School of Nursing and Health Professions, Georgia State University, Atlanta, GA, [¶]Departments of Physiology & Biophysics, Case Western Reserve University, Cleveland, OH, [**]Department of Neuroscience, School of Nursing, Case Western Reserve University, Cleveland, OH, [††]Department of Physiology, and [‡‡]Department of Psychiatry and Behavioral Sciences, Emory University, Atlanta, GA, USA
[1] These authors contributed equally to this study.

**Corresponding author: N. T. Sawyer, PhD, Department of Biology, Clayton State University, 2000 Clayton State Boulevard, Morrow, GA 30260, USA. E-mail: NikkiSawyer@clayton.edu*

Received 27 July 2015, revised 14 October, 18 December 2015, accepted for publication 18 December 2015

Mutations in the voltage-gated sodium channel gene *SCN1A* are responsible for a number of epilepsy disorders, including genetic epilepsy with febrile seizures plus (GEFS+) and Dravet syndrome. In addition, dysfunction in *SCN1A* is increasingly being linked to neuropsychiatric abnormalities, social deficits and cognitive disabilities. We have previously reported that mice heterozygous for the *SCN1A* R1648H mutation identified in a GEFS+ family have infrequent spontaneous seizures, increased susceptibility to chemically and hyperthermia-induced generalized seizures and sleep abnormalities. In this study, we characterized the behavior of heterozygous mice expressing the *SCN1A* R1648H mutation (*Scn1a*$^{RH/+}$) and the effect of stress on spontaneous and induced seizures. We also examined the effect of the R1648H mutation on the hypothalamic–pituitary–adrenal (HPA) axis response. We confirmed our previous finding that *Scn1a*$^{RH/+}$ mutants are hyperactive, and also identified deficits in social behavior, spatial memory, cued fear conditioning, pre-pulse inhibition and risk assessment. Furthermore, while exposure to a stressor did increase seizure susceptibility, the effect seen in the *Scn1a*$^{RH/+}$ mutants was similar to that seen in wild-type littermates. In addition, *Scn1a* dysfunction does not appear to alter HPA axis function in adult animals. Our results suggest that the behavioral abnormalities associated with *Scn1a* dysfunction encompass a wider range of phenotypes than previously reported and factors such as stress exposure may alter disease severity in patients with *SCN1A* mutations.

Keywords: Behavior, epilepsy, hyperactivity, *Scn1a*, sodium channel, stress

Mutations in the voltage-gated sodium channel (VGSC) gene *SCN1A* are responsible for several epilepsy subtypes, including Dravet syndrome (DS) (Claes *et al.* 2001), genetic epilepsy with febrile seizures plus (GEFS+) (Escayg *et al.* 2000) and intractable childhood epilepsy with generalized tonic-clonic seizures (GTCSs) (Fujiwara 2006; Mulley *et al.* 2005). The prevailing hypothesis that these mutations lead to seizure generation by reducing the excitability of inhibitory interneurons and thereby decreasing overall network inhibition (Martin *et al.* 2010; Ragsdale 2008; Tang *et al.* 2009; Yu *et al.* 2006) has recently been confirmed by studies directly linking the activity of *Scn1a* in parvalbumin interneurons to seizure susceptibility (Cheah *et al.* 2012; Dutton *et al.* 2013; Ogiwara *et al.* 2007). DS is characterized by febrile seizures in the first year of life, with progression to partial and/or generalized afebrile epilepsy, moderate to severe intellectual disability and ataxia (Fujiwara 2006; Mulley *et al.* 2005; Wolff *et al.* 2006). The less severe GEFS+ phenotype includes febrile seizures that persist beyond 6 years of age and the development of afebrile generalized or partial seizures during adulthood (Scheffer & Berkovic 1997). Within a GEFS+ family, affected members with the same mutation exhibit a wide range of epilepsy subtypes and severities, suggesting that other genetic, developmental and/or environmental factors may play a role in the development and expression of GEFS+ (Scheffer & Berkovic 1997). There is anecdotal evidence to suggest that stress can precipitate seizures in some patients with GEFS+ (Baulac *et al.* 2008; Grant & Vazquez 2005), and the avoidance of stressful situations is recommended for DS patients (Ceulemans *et al.* 2004).

In addition to epilepsy, some individuals with *SCN1A* mutations display neuropsychiatric abnormalities, such as anxiety and affective disorders and autism (Mahoney *et al.* 2009; O'roak *et al.* 2012; Osaka *et al.* 2007; Weiss *et al.* 2003), suggesting that a wider range of phenotypes are associated with *SCN1A* mutations. Autism spectrum disorders have been more broadly linked with deficiencies in inhibitory signaling (Chao *et al.* 2010; Paluszkiewicz *et al.* 2011), possibly providing a mechanistic basis for the relationship with altered *SCN1A* function. Autistic-like behaviors have also been described in two loss-of-function *Scn1a* mouse mutants that model DS (Han *et al.* 2012; Ito *et al.* 2012), providing further support for a link between *SCN1A* dysfunction and autistic-like behaviors.

The *SCN1A* mutation, R1648H, was identified in a large family with GEFS+ (Escayg *et al.* 2000). We previously

reported the generation of a mouse model of GEFS+ by knocking in the R1648H mutation into the orthologous mouse *Scn1a* gene (Martin *et al.* 2010). Heterozygous mutants (*Scn1a*$^{RH/+}$) exhibit infrequent spontaneous generalized seizures and lower thresholds to flurothyl- and hyperthermia-induced seizures, whereas homozygous mutants (*Scn1a*$^{RH/RH}$) exhibit frequent spontaneous seizures and premature lethality. We have also observed sleep abnormalities in the *Scn1a*$^{RH/+}$ mutants (Papale *et al.* 2013), further expanding the range of clinical phenotypes that may be associated with *SCN1A* dysfunction. Previous work on *Scn1a*$^{RH/+}$ mutants was performed in mice on a mixed 129X1/SvJ × C57BL/6J background (N2 generation). To reduce the influence of the mixed genetic background on observed phenotypes, we backcrossed the *Scn1a*$^{RH/+}$ line to C57BL/6J for 12 generations (N12) prior to inclusion in this study.

The goal of this study was threefold. First, we examined the behavioral characteristics of the *Scn1a*$^{RH/+}$ mutants. Second, we examined the effect of stress on seizure occurrence and asked if the *Scn1a*$^{RH/+}$ mutation was sufficient to alter the functioning of the hypothalamic–pituitary–adrenal (HPA) axis, a key player in the physiological stress response. Finally, we re-examined the influence of the *Scn1a* R1648H mutation on seizure threshold and life span in mice at the N12 generation.

Methods

Animals

Scn1a^{RH} mice were generated as previously described (Martin *et al.* 2010). *Scn1a*$^{RH/+}$ males were backcrossed to C57BL/6J females to advance to the 12th generation on the C57BL/6J background, designated as N12. Survival and pre-weaning weights were monitored for one cohort of males and females and then combined after verifying a lack of sex effects prior to weaning. Additional male mice, 3–4 months old, were used for all other experiments. The same cohort of male animals was used for object recognition, visual cliff and mating call experiments (in that order), with 2 weeks separating each paradigm in order to reduce stress effects. A different cohort of male animals was used for social interaction, startle/pre-pulse inhibition (PPI) and fear conditioning experiments (in that order), with 2 weeks separating each paradigm. All other experiments were each completed with different cohorts of male animals. Wild-type (WT) littermates were used as controls for all experiments to minimize variation. Mice were group-housed after weaning (P21) in ventilated cages under uniform conditions with a 12/12 h light/dark cycle with lights on at 0700 h and lights off at 1900 h. Mice remained group-housed until 1 week prior to testing, at which time they were single-housed. Food and water were available *ad libitum*. All testing was performed between 0800 and 1300 h to minimize variation owing to circadian factors. All videotaped behaviors and electroencephalogram (EEG) data were later scored by a single observer for each experiment who was blind to genotype and condition. All experiments were approved by the Emory University Institutional Animal Care and Use Committee (IACUC).

Genotyping

Genotyping of *Scn1a*^{RH} mutants was performed as previously described (Martin *et al.* 2010). Heterozygous *Scn1a*$^{RH/+}$ mutants were identified by the presence of both a WT band and a mutant band. Homozygous *Scn1a*$^{RH/RH}$ mutants were identified by the absence of the WT band.

Life span and weights

To characterize the effect of the *Scn1a* R1648H mutation on the C57BL/6J background, 20 WT C57BL/6J females were bred with two different heterozygous *Scn1a*$^{RH/+}$ males (N11 generation) to obtain 20 litters of N12 offspring ($n = 146$ offspring). The litters comprised on average 7.3 pups per litter, with expected Mendelian ratios for the offspring. Beginning on postnatal day 2 (P2), all pups were weighed daily until weaning (P21) and then weekly until postnatal week 8 with one final weight measurement on postnatal day 90. All mice were monitored daily from P2 until P90.

Stressor

Mice were placed into adequately ventilated clear polypropylene restrainers (50-ml conical tubes measuring 9.7 cm in length with an internal diameter of 2.8 cm) for 20 min. Breathing was carefully observed to ensure the animals were not compressed.

EEG analysis of spontaneous seizure activity

Under isoflurane anesthesia, eight male *Scn1a*$^{RH/+}$ mutants were surgically implanted with EEG and electromyography (EMG) electrodes for seizure monitoring as previously described (Papale *et al.* 2010). Following 7 days of recovery, the animals were single-housed in Plexiglas boxes ($20 \times 20 \times 30$ cm^3), and following an additional 24 h of habituation, continuous EEG and EMG data along with simultaneous digital video recording were collected for 7 days. Data were analyzed for the number of seizures as characterized by polyspike activity accompanied by stereotypic seizure behaviors and a refractory period. Specifically, epileptiform activity was characterized by the onset of sharp waves that increased in frequency and achieved amplitudes that were at least two times the background with detection in all cortical EEG channels and attenuation of the background rhythm (see Video S1, Supporting information). Following the 7-day period of baseline recording, the effect of acute restraint stress on spontaneous seizure frequency was determined by placing animals into modified restraint tubes (50-ml conical plastic tube with a 1.5×1.5 cm^2 hole cut out for EEG headcap placement) for 20 min. Continuous EEG data were collected during restraint as well as for the 6-day period following the acute restraint. The effect of chronic restraint stress on spontaneous seizure frequency was then determined by placing the same animals into modified restraint tubes for 20 min each day over a 6-day period. EEG data were collected for an additional 4 days after the completion of stress exposure on the sixth day.

Flurothyl seizure induction

Flurothyl seizure induction was performed as previously described (Dutton *et al.* 2011; Martin *et al.* 2007). Briefly, mice (14 *Scn1a*$^{RH/+}$ and 15 WT littermates) were placed into a clear acrylic chamber and exposed to flurothyl (2,2,2-trifluroethylether) (Sigma-Aldrich, St. Louis, MO, USA) at a rate of 20 μl/min. The latencies to the first myoclonic jerk (MJ) and to the GTCS were recorded.

Picrotoxin seizure induction

Mice (24 *Scn1a*$^{RH/+}$ mutants and 24 WT littermates) were acclimated in the procedure room 2 h prior to the experiment. Twelve mice of each genotype were subjected to an acute 20-min restraint stress just prior to injection, while the other twelve served as unstressed controls. Mice were injected intraperitoneally with 5 mg/kg picrotoxin (Sigma-Aldrich, St. Louis, MO, USA) dissolved in 0.9% saline and videotaped to monitor seizure phenotypes for 1 h post-injection. Picrotoxin-induced seizure activity was scored based on the following criteria recommended for seizures induced by disruption of the GABAergic system (Veliskova 2006): 0, no behavioral response; 0.5, abnormal behavior (freezing, staring and orientation problems); 1, isolated MJs; 2, atypical clonic seizure; 3, fully developed bilateral forelimb clonus; 3.5, forelimb clonus with a tonic component and twist of the body; 4, GTCS with a suppressed tonic phase and 5, fully developed GTCS with hindlimb extension. Because the stages of seizure activity owing to GABAergic disruption represent a progression of seizure activity that spreads from the forebrain to the

brainstem (Veliskova 2006), animals that exhibited rapid progression to higher levels of seizure activity without overtly displaying the characteristic seizure responses of lower stages were scored as progressing through all previous stages of seizure activity. Discrete stage 4 seizure events were defined as being a GTCS with loss of righting reflex followed by a period of rest and return of the righting reflex. Seizures were scored by an observer who had previously observed picrotoxin-induced behavioral seizure activity during simultaneous EEG recording.

Open field test

The open field apparatus consisted of a square arena (60×60 cm^2) with opaque Plexiglas walls (47 cm high). The arena was brightly lit with overhead fluorescent lighting (1000 lux). The center zone was designated as a smaller square (30×30 cm^2). Twelve mice from each genotype were tested. Each mouse was placed along one side of the apparatus and allowed to explore for 15 min. Mice were videotaped and behavior was scored using the ANY-maze Video Tracking System (Stoelting Co, Wood Dale, IL, USA). Behaviors scored included time spent in the center zone, latency to enter the center zone, total distance traveled, average speed and total time spent immobile.

Object recognition test

Testing was conducted in the open field square arena (60×60 cm^2). A total of four different shaped and colored plastic objects (similar in size, $\sim 10 \times 6 \times 6$ cm^3, but different in texture) were used for testing. The test session consisted of four consecutive trials, each 10 min in duration with 5-min breaks between trials. Twelve mice of each genotype were tested. In trial 1, the mouse was placed in the center of the empty open field and allowed to freely explore the testing arena. For trial 2, three objects were introduced into the open field in three designated locations at least 5 cm from the walls. The selection of the objects and their placement within the open field was randomized for each mouse. For trial 3, one object from trial 2 was replaced with a novel object in the same location (novel object). In trial 4, a different object from trial 2 was relocated to a novel fourth location (relocated object). Throughout trials 2, 3 and 4, there was one object that was never changed nor moved (control object). Mice were videotaped and behavior was scored using the ANY-maze Video Tracking System (Stoelting Co). The time spent exploring each object within the first 5 min of the trial was scored. A mouse was considered to be exploring an object when it was facing the object at a close distance (≤5 mm) or when the mouse's nose or front paws were in contact with the object. To evaluate object recognition memory, the discrimination ratio was calculated by taking the time spent in trial 3 exploring the novel object and dividing it by the total time spent exploring the novel and the control object (*i.e.* novel/(novel + control) × 100). This score provides a measurement of the subject's memory for an object's identity, and since mice have an innate preference for novelty (Antunes & Biala 2012), it is expected that they will spend more time with the novel object (a ratio significantly >50%). Similarly, to evaluate spatial object memory, the discrimination ratio was calculated by taking the time spent in trial 4 exploring the relocated object and dividing it by the total time spent exploring the relocated and the control object (*i.e.* relocated/(relocated + control) × 100). As described before, a score significantly >50% would demonstrate memory of the object's original spatial position.

Contextual and cued fear conditioning

On the first day, mice (12 *Scn1a*$^{RH/+}$ and 12 WT littermates) were placed into a fear conditioning apparatus [$17.5 \times 17.5 \times 30$ cm^3; Colbourn, Whitehall, PA, USA] and allowed to explore the enclosure for 3 min. Following this habituation period, three conditioned stimulus (CS)–unconditioned stimulus (US) pairings were presented with a 1-min intertrial interval. The CS consisted of a 20-second 85-dB tone and the US consisted of 2 seconds of a 0.5-mA footshock which co-terminated with each CS presentation. Shock was delivered via a Precision Animal Shocker (Colbourn) connected to the fear conditioning chamber. One minute following the last CS–US presentation, animals were returned to their home cage. On day 2, mice were tested for contextual fear conditioning by placing them into the same chamber used for conditioning on day 1 for 8 min with no shocks. On day 3, mice were tested for cued fear conditioning by placing them into a novel compartment and first allowing them to freely explore the novel context for 2 min. Following this habituation period, the CS (85 dB tone) was presented for 6 min. No shocks were administered during the tone test. During all 3 days, animals were recorded via a camera and the amount of freezing was measured using software provided by Colbourn.

Baseline startle and PPI

Startle was measured using a San Diego Instruments SR-Lab Startle Response System (San Diego, CA, USA). Mice (12 *Scn1a*$^{RH/+}$ and 12 WT littermates) were placed into the Plexiglas holders and allowed to acclimate to the chamber and background white noise (60 dB) for 5 min. After the acclimation period, randomized trials of either startle alone (117 dB for 40 milliseconds), no stimulus (background noise only), or startle preceded by one of the four pre-pulse intensities (70, 72, 76 or 80 dB) were administered. A total of 48 trials were run (eight trials of each of the different conditions) with a random intertrial interval. The maximum startle amplitude was measured during the first 100 milliseconds following the pulse presentation for each trial. The average startle amplitude of the combination of the pre-pulse paired with the pulse relative to the startle response alone was used to calculate the PPI.

Predator odor exposure

Predator odor exposure occurred in an enclosed transparent box ($30 \times 30 \times 30$ cm^3). Separate, yet identical, boxes were used for odor exposure and vehicle exposure to prevent any residual odor from affecting the control exposures. The boxes were placed in a ventilated hood to allow for adequate disposition of the odor. Synthetic fox feces odor, 2,5-dihydro-2,4,5-trimethylthiazoline (TMT; Contech, Victoria, Canada), was diluted 1:100 in ethanol. On the first day, animals (10 *Scn1a*$^{RH/+}$ and 10 WT littermates) were placed into the control box, and 35 μl of vehicle (ethanol) was placed on a small piece of filter paper (placed on a small shelf). The box was then closed, and the animal was observed and videotaped for 15 min. After 48 hours, the animal was placed into the odor box, and 35 μl of diluted TMT was placed on the filter paper. The animal was again observed and videotaped for 15 min. After an additional 48-h period, the animal was returned to the odor box with 35 μl of vehicle to determine if contextual fear memories were formed. Mice were scored for total freezing time (defined as the lack of movement except for respiration and heart beat) and number of rearing occurrences.

Olfactory discrimination tests

The ability to detect three types of odors (food, social and aversive) was tested using a three-chambered apparatus with small openings in each partition (5×5 cm^2). Each of the three chambers measured $20 \times 40 \times 22$ cm^3 (h). A covered Petri dish with holes to release the odor was used to hold the odors and the control odor (water). Each test involved the placement of different materials into the test dish: mix of seed and nuts (food test) (Kaytee, Chilton, WI, USA); soiled bedding from an unfamiliar male mouse (social test); or 10 μl of diluted TMT (aversive test). The test dish was placed in the corner in one of the outer chambers, and the control dish containing water was placed in the corner in the opposite outer chamber. Animals (12 *Scn1a*$^{RH/+}$ mutants and 12 WT littermates) were placed into the middle chamber and allowed to freely explore for 10 min. Animals were videotaped, and the video was later scored using the ANY-Maze Video Tracking System (Stoelting Co). For the food and social odors, the time spent in a 6-cm zone around the two dishes was scored. For the aversive odor, a transparent Plexiglas lid was placed over the chamber to minimize diffusion of the highly volatile TMT throughout the chamber. Analysis of the aversive odor was carried out by calculating the percent of time spent in the chamber containing the aversive odor as compared with the time spent in the other two chambers. A score of 33.3% would represent chance occurrence.

Visual cliff avoidance task

The visual cliff avoidance task was conducted in a rectangular clear Plexiglas box with a clear bottom. White paper was taped around the sides to make them opaque and to prevent the mouse from seeing the behavioral test administrator in the room. The box was secured so that half of the floor of the box overhung the table top to create the appearance of a ledge drop-off. A checkerboard tablecloth draped from the table top to the floor served to enhance the visual appearance of the cliff. An opaque neutral zone ($10 \times 10\,cm^2$) was located in the center of the box floor. The side overhanging the table top was designated as the 'cliff' zone and the side sitting on the table was designated as the 'safe' zone. The neutral zone lay between the cliff zone and safe zone. Mice (12 *Scn1a*$^{RH/+}$ mutants and 12 WT littermates) were placed onto the neutral central region and allowed to freely explore for 10 min. Mice were recorded and the video was analyzed using the ANY-Maze Video Tracking System (Stoelting Co). The time spent in each zone and the time spent in the center of the cliff zone, designated as the area of the cliff zone at least 6 cm away from any wall, were measured.

Vision testing

Visual function was tested using the virtual optokinetic system (OptoMotry system; Cerebral Mechanics, Lethbridge, Canada) as previously described (Douglas *et al.* 2005). Briefly, the mice (five *Scn1a*$^{RH/+}$ mutants and five WT littermates) were placed on a platform at the center of a virtual reality chamber composed of four computer monitors that display vertical sine wave grating rotating at a speed of 12°/second. The experimenter monitored the mice in real-time through a video camera situated above the animal and noted the presence or absence of reflexive head movements (tracking) to the gratings. The experimenter also manually tracked the head of the mouse to align the center of the virtual cylinder to the viewing position of the mouse. For visual acuity assessment, the grating started at a spatial frequency of 0.042 cycles/degree with 100% contrast and increased with a staircase procedure. The maximum spatial frequency capable of eliciting head tracking was determined using the OptoMotry system (Cerebral-Mechanics).

Social interaction

Social interaction was tested using the same three-chambered apparatus described in the preceding *Olfactory discrimination test* section. A cylindrical wire cage (10 cm diameter, Pencil Holder, Design Ideas, Springfield, IL, USA) was used as an inanimate object or the cage housing a stranger mouse. In the first 10-min session, a test mouse (12 *Scn1a*$^{RH/+}$ mutants and 12 WT littermates) was placed in the center chamber and allowed to freely explore. In the second 10-min session, an age- and sex-matched C57BL/6J mouse (stranger) that had never been exposed to the test mouse was placed in one of the two wire cages. The wire cage on the other side remained empty. For the third 10-min session, a second age- and sex-matched C57BL/6J stranger mouse (novel mouse) was placed in the wire cage that previously served as an empty cage, allowing the test mouse to have a choice between a familiar mouse and a novel mouse. All three stages were videotaped, and the video was analyzed using the ANY-Maze Video Tracking System (Stoelting Co). Time spent in each chamber and time spent within a 5-cm radius proximal to each wire cage were measured.

Mating calls

The home cages of male mice (12 *Scn1a*$^{RH/+}$ mutants and 12 WT littermates) were placed in a single-walled, $127 \times 83.8 \times 83.8\,cm^3$ sound-attenuating box (ETS-Lindgren, Cedar Park, TX, USA) with the lids removed. A Bruel & Kjær (Nærum, Denmark) microphone with a 1/4″ membrane diameter was positioned over the cage, 15 cm above the cage floor, with the membrane pointed downward into the cage. Under red light, animals were monitored from outside the sound box via a video camera and bat detector (Ultra Sound Advice, London, UK). After a 1-min period of baseline recording, an unfamiliar adult female mouse was introduced to the cage and animals were allowed to freely interact. Vocalizations were recorded at 223 kilosamples/second using Tucker-David Technologies data acquisition hardware (Alachua, FL, USA). After 10 min, the cage was removed from the sound box and the mice were separated. Vocalizations were extracted from the sound recordings offline, using custom MATLAB programs. After extraneous background noises were eliminated, putative calls (at least 5 milliseconds in length) were determined by identifying regions where the power exceeded a manually set threshold (set per animal by an experimenter blind to the animal's genotype). If consecutive calls were separated by fewer than 30 milliseconds, they were grouped as one. Although extraction was performed in an automated fashion, an experimenter validated call boundaries by visualizing spectrograms of a portion of the extracted calls.

Corticosterone measurements

Blood was collected at 0700 and 1900 h on two different days in order to coincide with the expected nadir and peak of circulating corticosterone (CORT) levels. A week after the last diurnal blood draw, the effect of a stressor on immediate CORT levels and on evening CORT levels was measured. Animals were subjected to a 20-min acute restraint stress in the morning between 0800 and 0900 h. Blood was drawn immediately after the restraint stress and then again at 1900 h for a post-stress evening CORT measurement. For all basal CORT measurements, blood was obtained within 1 min of cage disturbance. Blood was collected from the facial vein into Microvette CB 300 Z tubes (Starstedt, Numbrecht, Germany) and then allowed to clot for 1 h at room temperature. The serum was then separated by centrifugation at 5600 rpm ($2900 \times g$) for 15 min at 4°C and stored at −80°C until analysis. Serum CORT levels for the diurnal blood draws were assayed using a commercial radioimmunoassay kit (MP Biomedicals, Santa Ana, CA, USA) according to the manufacturer's instructions.

Statistics

The data are reported as mean ± SEM. When making *a priori* comparisons between only two groups of unrelated parametric data, the data were analyzed using the Student's *t*-test. In tests comparing a specific response to the response expected by chance, a one-tailed *t*-test was used. Parametric datasets with two or more groups/factors to be compared were analyzed using two-way analysis of variance (ANOVA) if there was only one measurement per animal or two-way repeated measures ANOVA (RANOVA) if there were multiple data values from a single animal. Following the ANOVAs, the Tukey pairwise comparison test was used to further distinguish among groups in cases where there was a significant main effect of one or both factors. *Post hoc* comparisons were also made in the absence of a significant interaction between the two main factors, as the error rate (alpha, α) is still properly controlled with multiple *post hoc* comparisons even in the absence of a significant interaction (Hancock & Klockars 1996; Ware *et al.* 2012). Nonparametric data were analyzed using the Mann–Whitney rank sum test. Dichotomous data were analyzed using the Fisher exact test. All results were considered statistically significant if $P < 0.05$.

Results

Scn1a$^{RH/+}$ mutants are hyperactive but show no deficits in anxiety

We have previously shown that *Scn1a*$^{RH/+}$ mutants have increased locomotor activity in a novel environment (Purcell *et al.* 2013). We have extended this finding to show that the *Scn1a*$^{RH/+}$ mutant mice show hyperactivity in the open field test. In the open field test, *Scn1a*$^{RH/+}$ mutants travel a greater total distance (*Scn1a*$^{RH/+}$, 88.9 ± 4.2 m; WT, 73.3 ± 4.1 m; $t_{21} = -2.649$, $P < 0.05$; Fig. 1a), travel at a higher average speed (*Scn1a*$^{RH/+}$, 9.9 ± 0.5 cm/second;

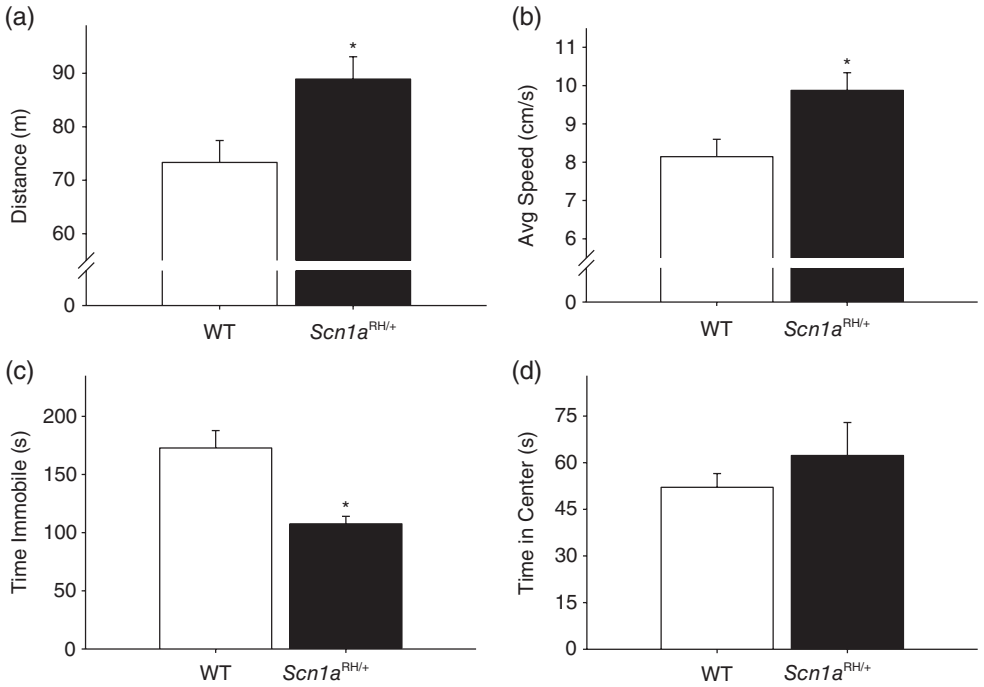

Figure 1: *Scn1a*$^{RH/+}$ mutants are hyperactive. *Scn1a*$^{RH/+}$ mutants (a) travel a greater distance, (b) travel at a higher average speed and (c) spend less time immobile while in the open field as compared with WT littermates. (d) There are no differences between genotypes in the time spent in the center zone of the open field. $n = 12$ all groups; $^*P < 0.05$ vs. WT; Error bars represent SEM.

WT, 8.1 ± 0.5 cm/second; $t_{21} = -2.665$, $P < 0.05$; Fig. 1b) and spend less time immobile during the task (*Scn1a*$^{RH/+}$, 107.6 ± 6.4 seconds; WT, 172.8 ± 15.0 seconds; $t_{21} = 3.867$, $P < 0.001$; Fig. 1c) as compared with WT littermates. There were no significant differences in the amount of time the *Scn1a*$^{RH/+}$ mutants spent in the center zone as compared with WT littermates (Fig. 1d), nor was there a difference in latency to enter the center zone (data not shown), suggesting that the mutants exhibit normal anxiety levels.

Scn1a$^{RH/+}$ mutants show mild cognitive impairment and deficits in sensorimotor gating

An object recognition test was used to assess learning and memory in the *Scn1a*$^{RH/+}$ mutants. While there was a statistically significant difference in the total distance traveled between *Scn1a*$^{RH/+}$ mutants and WT littermates during trial 1 (habituation to the open field; data not shown) confirming the aforementioned open field test findings, there were no differences in activity levels between the mutants and WT littermates during trials 2, 3 or 4 of the object recognition test (data not shown). Both *Scn1a*$^{RH/+}$ mutants and WT littermates spent more time with the novel object compared with the control object (one-tailed *t*-test, WT: $t_{11} = 8.452$, $P < 0.001$; *Scn1a*$^{RH/+}$: $t_{11} = 2.839$, $P < 0.05$; Fig. 2a). While the WT littermates spent a greater percentage of time with the novel object than the *Scn1a*$^{RH/+}$ mutants (WT: $74.4 \pm 2.9\%$; *Scn1a*$^{RH/+}$: $65.2 \pm 5.3\%$), the difference between genotypes did not reach statistical significance ($t_{22} = 1.519$, $P = 0.143$).

Mice have been shown to be able to form memories of not only the objects themselves, but also their location in space (Dere *et al.* 2005). Our results show that the WT animals, but not the *Scn1a*$^{RH/+}$ mutants, are able to remember the spatial location of the objects (one-tailed *t*-test, WT: $63.3\% \pm 5.7\%$, $t_{11} = 2.349$, $P < 0.05$; *Scn1a*$^{RH/+}$: $56.2\% \pm 6.8\%$, $t_{10} = 0.917$, $P = 0.381$; Fig. 2a). Thus, while both groups appear to remember the objects' identities equally well, the mutants show a deficit in spatial learning and memory in this task.

We also tested the *Scn1a*$^{RH/+}$ mutants with a fear conditioning paradigm. There were no differences between mutants and WT littermates in the time spent freezing on the day of training ($F_{6,132} = 1.343$, $P = 0.259$; Fig. 2b). There were also no differences between *Scn1a*$^{RH/+}$ mutants and WT littermates in the amount of freezing during the contextual fear conditioning component of the task (*Scn1a*$^{RH/+}$, $17.4\% \pm 2.5\%$; WT, $17.7\% \pm 1.3\%$; $t_{22} = 0.113$, $P = 0.911$; Fig. 2c, context). During the cued fear conditioning component, *Scn1a*$^{RH/+}$ mice froze significantly more in response to the CS than the WT littermates (*Scn1a*$^{RH/+}$, $63.0\% \pm 3.5\%$; WT, $45.8\% \pm 3.0\%$; $t_{22} = -3.700$, $P < 0.01$; Fig. 2c, cue). Closer examination of the time course of the cued fear conditioning task showed that the *Scn1a*$^{RH/+}$ mutants had a similar initial response to the tone as the WT littermates, but while the WT littermates show a steady decline in the amount of freezing over the 6 min of tone presentation, freezing levels remain elevated in the *Scn1a*$^{RH/+}$

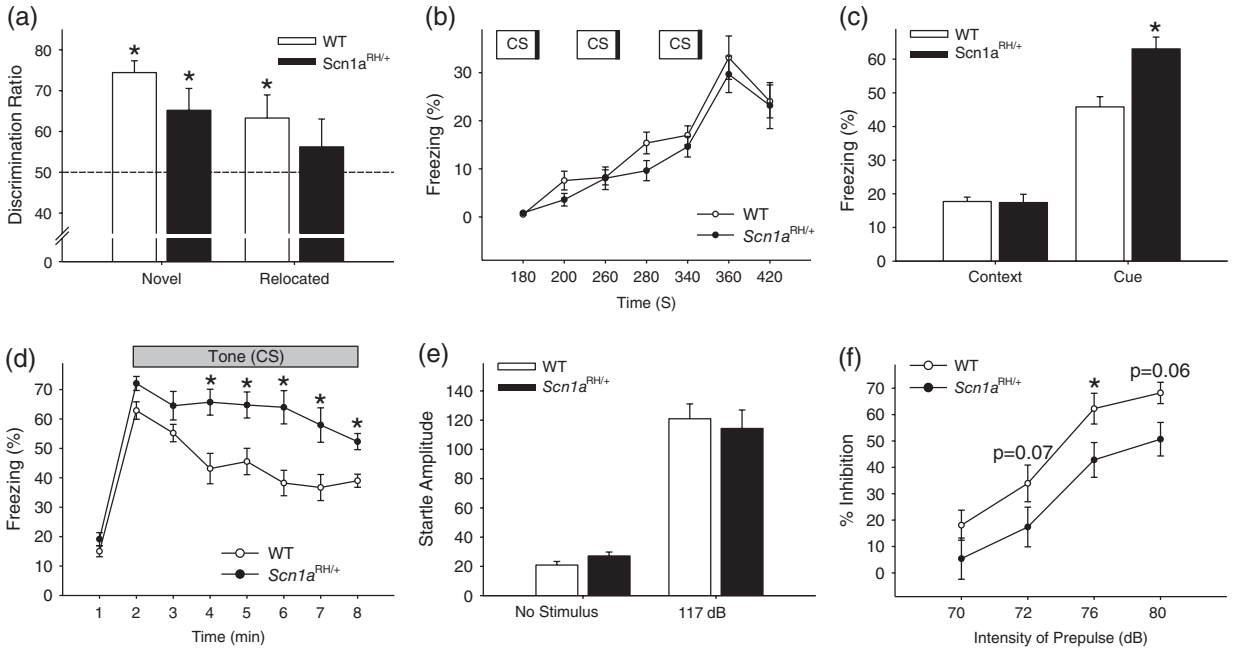

Figure 2: *Scn1a*$^{RH/+}$ mutants show mild cognitive deficits and impairments in sensorimotor gating. (a) Both *Scn1a*$^{RH/+}$ mutants and WT littermates show a preference for a novel object, but only the WT littermates show a preference for a relocated object. The value shown is the discrimination ratio, calculated as the time spent exploring the novel or relocated object divided by the total time exploring both the manipulated object and the control object, multiplied by 100. The dotted line represents a performance at chance level (50%). $*P < 0.05$, one-tailed *t*-test vs. 50% chance. (b) Both genotypes exhibited similar amounts of freezing during fear conditioning training which consisted of three CS–US (footshock, black line) pairings with a 1-min intertrial interval. (c) A contextual and cued fear conditioning task showed no differences in contextual freezing between *Scn1a*$^{RH/+}$ mutants and WT littermates, but *Scn1a*$^{RH/+}$ mutants showed significantly more cued freezing. $*P < 0.05$ vs. WT. (d) A closer examination of freezing during the cued fear conditioning paradigm shows that during the 6 min that the tone (CS) was played but no shock was administered, the WT littermates showed a reduction in their freezing behavior, while *Scn1a*$^{RH/+}$ mutants continued to maintain high levels of freezing. $*P < 0.05$ vs. WT. (e) There are no differences in the amplitude of the startle response between *Scn1a*$^{RH/+}$ mutants and WT littermates. (f) *Scn1a*$^{RH/+}$ mutants showed decreased PPI in the startle response compared with WT littermates, particularly at the higher decibel levels of the pre-pulse tone. $*P < 0.05$ vs. WT. $n = 12$ all groups. Error bars represent SEM.

mutants (Fig. 2d). A two-way RANOVA of the 6-min period of tone presentation shows a significant main effect of genotype ($F_{1,22} = 13.687$, $P < 0.01$), a significant main effect of time ($F_{6,132} = 13.813$, $P < 0.001$) and a significant interaction between genotype and time ($F_{6,132} = 2.689$, $P < 0.05$). *Post hoc* analysis (Tukey) shows a significant difference in freezing between *Scn1a*$^{RH/+}$ mutants and WT littermates during the last 4 min of the 6-min tone presentation (Fig. 2d).

To measure sensorimotor gating, we used a PPI paradigm. There were no differences in the startle amplitude between *Scn1a*$^{RH/+}$ mutants and WT littermates to a startle stimulus (117 dB) presented alone (Fig. 2e). However, *Scn1a*$^{RH/+}$ mutants show deficits in the ability of a pre-pulse to inhibit the startle response (Fig. 2f). As the intensity of the pre-pulse increases, the amount of inhibition of the startle response should also increase. This was true for both genotypes as indicated by a main effect of PPI intensity ($F_{3,66} = 45.417$, $P < 0.001$) and no genotype–intensity interaction. However, there was also a main effect of genotype ($F_{1,22} = 5.475$, $P < 0.05$), and *post hoc* analysis (Tukey) showed that there was a significant reduction in PPI at a 76-dB pre-pulse intensity level between mutants and WT littermates. There was also a strong trend for a reduction in PPI at the 72- and 80-dB pre-pulse intensity levels.

Scn1a$^{RH/+}$ mutants may show a deficit in risk assessment ability

We originally chose the predator odor paradigm to measure anxiety and fear behavior in the *Scn1a*$^{RH/+}$ mutants. Two-way RANOVA showed a significant main effect of genotype ($F_{1,18} = 5.876$, $P < 0.05$), a significant main effect of odor exposure ($F_{2,36} = 26.614$, $P < 0.001$) and a significant interaction between genotype and odor exposure ($F_{2,36} = 4.110$, $P < 0.05$). *Post hoc* analysis (Tukey) showed that only the WT littermates froze significantly more to odor exposure than they did to the first vehicle exposure (Fig. 3a). While both genotypes exhibited contextual fear memory by freezing more on the second vehicle exposure in the same context as the predator odor exposure 48 h earlier, the WT littermates again spent significantly more time freezing than the *Scn1a*$^{RH/+}$ mutants (Fig. 3a).

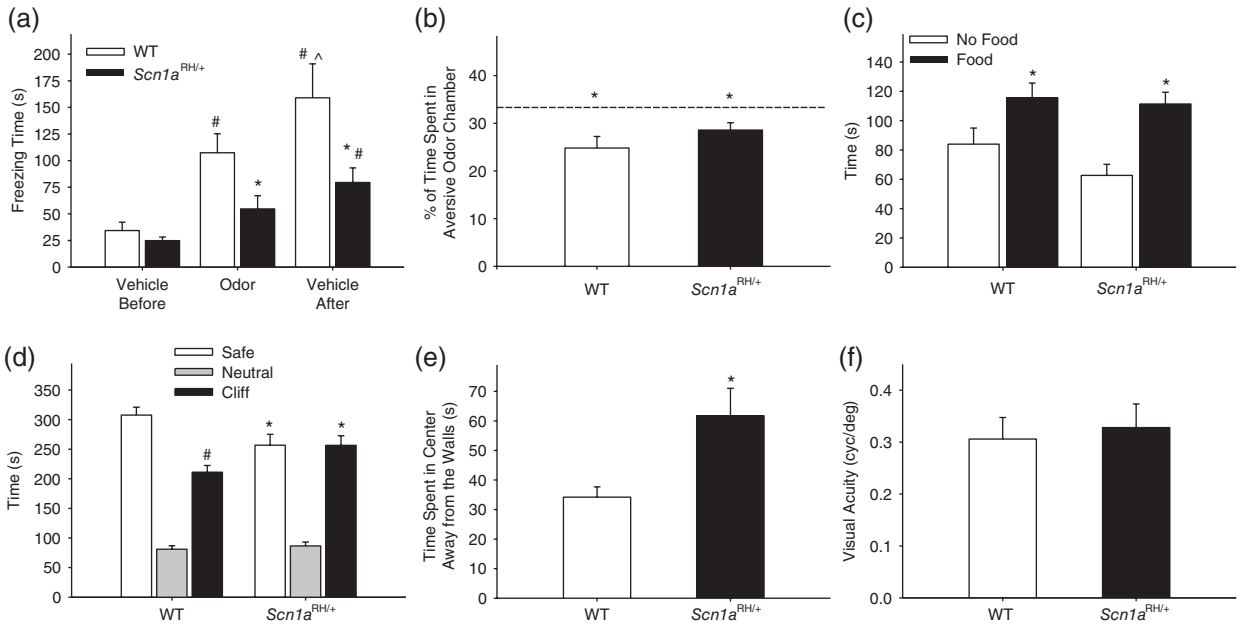

Figure 3: *Scn1a*$^{RH/+}$ mutants show deficits in risk assessment. (a) WT littermates, but not *Scn1a*$^{RH/+}$ mutants, froze significantly more during predator odor exposure when compared with previous exposure to vehicle (Vehicle Before). Both genotypes exhibited increased freezing 48 h later when exposed again to vehicle (Vehicle After), indicating formation of contextual fear memory, although the *Scn1a*$^{RH/+}$ mutants continued to freeze less than the WT littermates. *$P < 0.05$ vs. WT within Odor condition; #$P < 0.05$ vs. Vehicle Before within genotype; ^$P < 0.05$ vs. Odor within genotype. (b) The ability to detect an aversive odor was tested in a three-chambered apparatus. The percentage of time spent in the chamber containing the aversive odor was measured. A value of 33.3% represents chance (dotted line). Both *Scn1a*$^{RH/+}$ mutants and WT littermates spent significantly <33.3% of the time in the chamber with the aversive odor. *$P < 0.05$ one-tailed *t*-test vs. 33.3% chance. (c) The ability of *Scn1a*$^{RH/+}$ mutants to detect odor in general was tested using a novel food item. Both *Scn1a*$^{RH/+}$ mutants and WT littermates spent more time in the chamber containing the food item than in the chamber containing a control item. *$P < 0.05$ vs. control (no food). (d) During the visual cliff task, WT littermates spent less time on the side of the apparent cliff than on the safe side. However, *Scn1a*$^{RH/+}$ mutants do not differentiate the safe side from the cliff side. *$P < 0.05$ vs. WT within zone; #$P < 0.05$ vs. safe side within genotype. (e) A further examination of the visual cliff test shows that when the WT littermates are on the virtual cliff side of the apparatus they spend less time in the open center, away from the walls compared with *Scn1a*$^{RH/+}$ mutants. *$P < 0.05$ vs. WT. (f) In an analysis of visual acuity, there is no difference between *Scn1a*$^{RH/+}$ mutants and WT littermates. $n = 10–12$ all groups (a–e), $n = 5$ in both groups (f). Error bars represent SEM.

As the *Scn1a*$^{RH/+}$ mutants were freezing much less than WT littermates in response to the predator odor, we wanted to verify the olfactory ability in these mice. In an odor discrimination task using an aversive odor, both *Scn1a*$^{RH/+}$ mutants and WT littermates spent less time in the side of the apparatus where the aversive odor was located (Fig. 3b) than would be expected by chance in a three-chambered apparatus (33.3%). To further verify the olfactory ability, we also tested both groups with a positive odor (food). There was a main effect of food odor ($F_{1,22} = 14.280$, $P < 0.01$), and both *Scn1a*$^{RH/+}$ mutants and WT littermates spent more time in the chamber with the food than in the chamber without the food (Fig. 3c). As none of the other behavioral tasks had shown any measures of increased anxiety in the *Scn1a*$^{RH/+}$ mutants, and we had frequently observed the *Scn1a*$^{RH/+}$ mutants reacting differently from their WT littermates during routine colony procedures (personal observations), we wondered if the mutants had an impaired ability to assess risk.

To investigate the ability of the mutants to assess risk, we used a virtual cliff avoidance paradigm. The testing apparatus had a transparent bottom and was set up to overhang a table top to create the appearance of a sharp drop-off. The zone overhanging the table top was designated as the cliff zone and the zone on top of the table was designated as the safe zone. A narrow neutral zone separated these two zones. A two-way ANOVA showed a main effect of zone ($F_{2,44} = 86.604$, $P < 0.001$) and a significant genotype–zone interaction ($F_{2,44} = 4.745$, $P < 0.05$), indicating that the two genotypes were not responding to the zones in the same manner. *Post hoc* analysis (Tukey) showed that, as expected, the WT littermates spent more time in the safe zone than in the cliff zone (Fig. 3d). However, the *Scn1a*$^{RH/+}$ mutants showed no discrimination between the safe zone and the cliff zone. After noticing that some animals stayed close to the walls when venturing into the cliff zone while others went straight out over the apparent drop-off, we compared the amount of time that animals spent in the middle of the cliff zone away from the walls. *Scn1a*$^{RH/+}$ mutants spent significantly more time in the open center of the cliff zone as compared with WT littermates (*Scn1a*$^{RH/+}$,

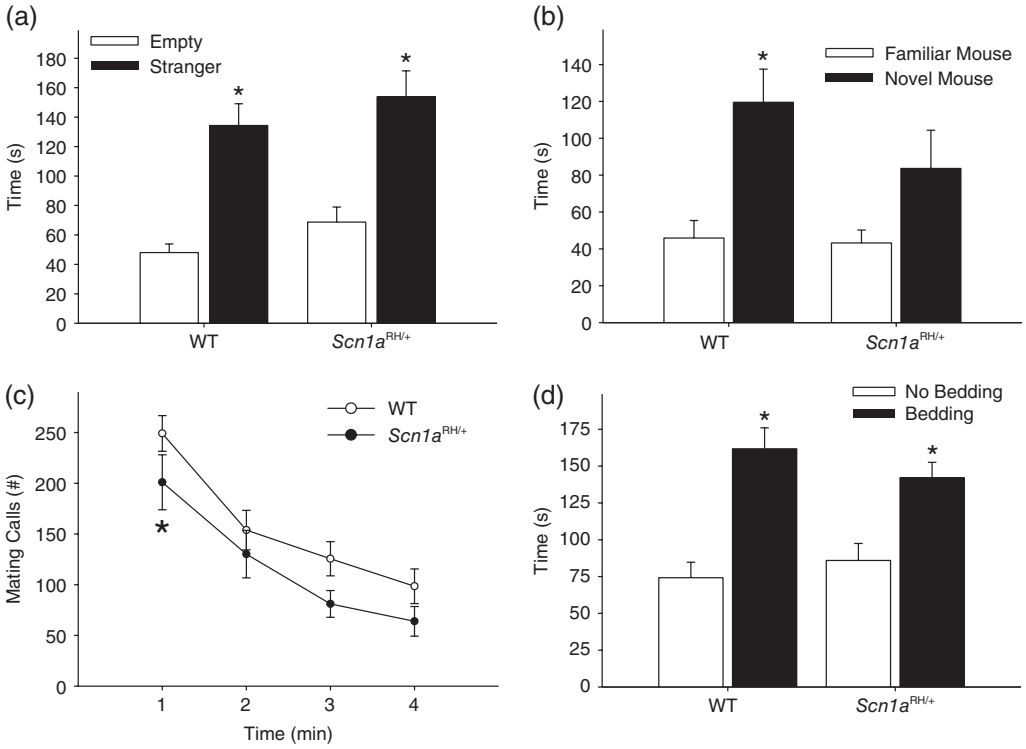

Figure 4: *Scn1a*$^{RH/+}$ mutants show mild social deficits. (a) In a choice between a chamber with an empty cage and a chamber with a cage housing a stranger mouse, both *Scn1a*$^{RH/+}$ mutants and WT littermates preferred to spend time with the stranger mouse. $*P < 0.05$ vs. empty chamber. (b) In a choice between a familiar mouse and a novel mouse, only the WT littermates showed a significant preference for the novel mouse. $*P < 0.05$ vs. familiar mouse. (c) When exposed to an unfamiliar female mouse, male mice exhibited numerous mating calls. In the first minute of exposure, WT littermates emitted more calls than the *Scn1a*$^{RH/+}$ mutants, and an overall main effect of genotype indicates that WT littermates are calling more in general than *Scn1a*$^{RH/+}$ mutants. $*P < 0.05$ vs. WT. (d) In an olfactory discrimination test using a socially relevant odor (soiled bedding), both *Scn1a*$^{RH/+}$ mutants and WT littermates showed a preference for the chamber containing the soiled bedding. $*P < 0.05$ vs. no bedding. $n = 12$ all groups. Error bars represent SEM.

61.8 ± 9.3 seconds; WT, 34.2 ± 3.5 seconds; $t_{22} = -2.774$, $P < 0.05$; Fig. 3e). This result suggested that either the *Scn1a*$^{RH/+}$ mutants could not see the virtual drop-off or they did not avoid it, possibly because of a lack of risk assessment ability. To ensure that the *Scn1a* mutation did not affect visual ability, we tested the visual acuity of both genotypes. There were no differences in visual acuity between *Scn1a*$^{RH/+}$ mutants and WT littermates in a vision function test (Fig. 3f).

Scn1a$^{RH/+}$ mutants show mild social deficits

In a three-chambered social task where mice had a choice between a stranger mouse and an empty cage (an inanimate object), both *Scn1a*$^{RH/+}$ mutants and WT littermates showed a preference for a stranger mouse over the empty cage (Fig. 4a). A two-way RANOVA showed only a significant main effect of the stranger mouse ($F_{1,22} = 42.524$, $P < 0.001$). There was no significant main effect of genotype nor interaction between genotype and stranger. The second task involved a choice between an already familiar mouse and a novel mouse. Again, there was a main effect of the novel mouse (Fig. 4b; $F_{1,20} = 10.707$, $P < 0.01$), but *post hoc* analysis showed that only the WT littermates had a significant preference for the novel mouse. During a mating call analysis paradigm, all males readily investigated the unfamiliar female mouse upon her introduction to the cage, and vocalizations were detected in all recordings. In an analysis of the first 4 min of exposure to the female, there was a strong trend for a main effect of genotype ($F_{1,21} = 4.211$, $P = 0.053$) and a significant main effect of time ($F_{3,63} = 48.417$, $P < 0.001$) indicating that the number of calls decreased as interaction time increased. *Post hoc* analysis showed a significant difference in calls during the first minute, with WT littermates emitting more calls than the *Scn1a*$^{RH/+}$ mutants (Fig. 4c). After the first 4 min of the test had elapsed, the number of calls had decreased dramatically and there were no longer any genotype differences (data not shown). Moreover, there were no significant genotype differences in mean call duration or mean call frequency (data not shown). Overall, during the first 4 min of interaction time, *Scn1a*$^{RH/+}$ mutants were emitting fewer calls than their WT littermates.

As part of a series of olfactory discrimination tasks, we tested the ability of *Scn1a*$^{RH/+}$ mutants to detect a socially relevant odor by placing soiled bedding from an unfamiliar male mouse into one chamber of the three-chambered apparatus.

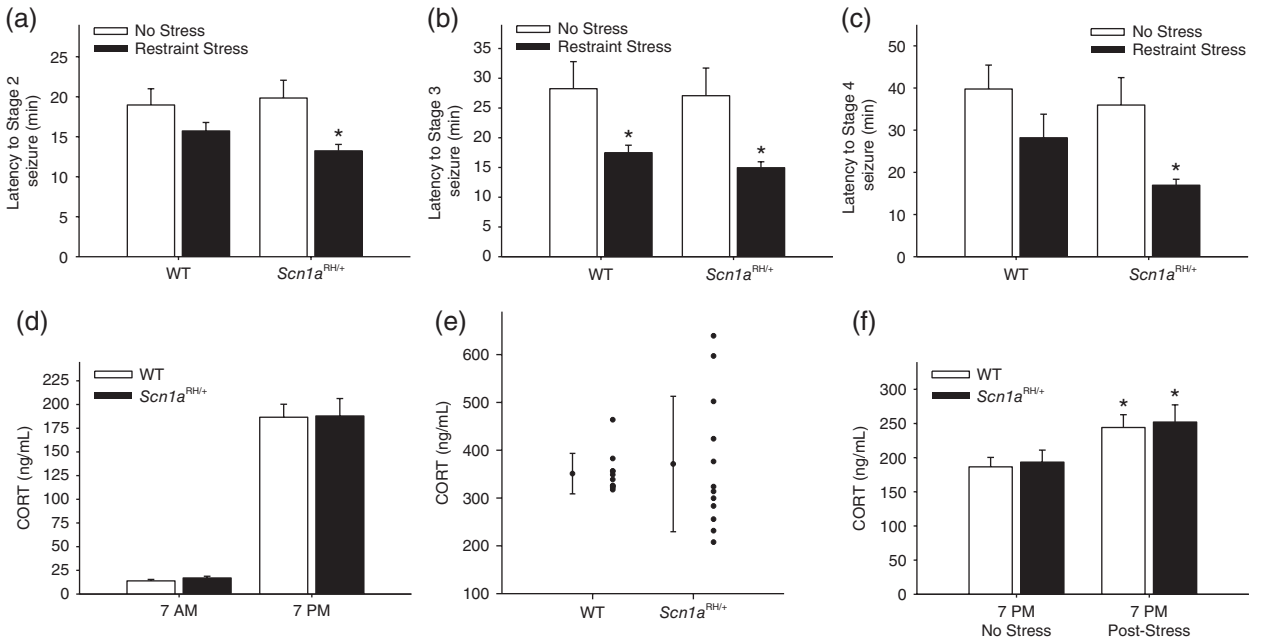

Figure 5: Stress worsens seizures in *Scn1a*$^{RH/+}$ mutants and WT littermates. (a) A 20-min acute restraint stress significantly reduced the latency to a stage 2 picrotoxin-induced seizure in *Scn1a*$^{RH/+}$ mutants, but not in WT littermates. $*P < 0.05$ vs. no stress. (b) Stress significantly decreased latency to a stage 3 picrotoxin-induced seizure in both *Scn1a*$^{RH/+}$ mutants and WT littermates. $*P < 0.05$ vs. no stress. (c) Stress significantly decreased the latency to a stage 4 picrotoxin-induced GTCS in *Scn1a*$^{RH/+}$ mutants while the *post hoc* results were not significant for WT littermates. $*P < 0.05$ vs. no stress. (d) *Scn1a*$^{RH/+}$ mutants have normal diurnal fluctuations in plasma CORT levels, with similar levels as WT littermates during both the nadir (0700 h) and peak (1900 h) of the circadian HPA axis rhythm. (e) Although the average CORT response to an acute 20-min restraint stress is not significantly different between genotypes, the *Scn1a*$^{RH/+}$ mutants exhibit more variability in their post-stress CORT levels. (f) Morning exposure to acute restraint stress increased CORT levels at 1900 h in both *Scn1a*$^{RH/+}$ mutants and WT littermates. $*P < 0.05$ vs. 1900 h no stress. $n = 12$ all groups. Error bars represent SEM.

Both *Scn1a*$^{RH/+}$ mutants and WT littermates spent more time in the chamber containing the bedding (Fig. 4d). There was a main effect of bedding odor ($F_{1,22} = 31.129$, $P < 0.001$) but no main effect of genotype nor genotype–odor interaction. This indicates that the *Scn1a*$^{RH/+}$ are responsive to socially relevant odors. Although the *Scn1a*$^{RH/+}$ mutants have a normal preference for social ability and a socially relevant odor, the reduced response to social novelty and the reduced number of mating calls suggests that the *Scn1a*$^{RH/+}$ have a mild social impairment.

Stress worsens seizure outcome in Scn1a$^{RH/+}$ *mutants and WT littermates*

We first analyzed the effects of acute restraint stress and chronic daily restraint stress on spontaneous seizure activity. The EEG analysis detected spontaneous seizures in two of the eight animals during the baseline recording period. Following chronic daily restraint stress (20-min restraint once a day for 6 days), these two mice began to have more frequent seizures, described as follows: Mouse #1 had an average of one seizure per day during baseline recordings yet exhibited between two and five seizures per day during and following chronic stress administration. Mouse #2 had only one seizure during the total baseline recording period but progressed to one seizure per day during and following chronic stress administration. The six non-seizing animals did not show any seizure activity following an acute or chronic stressor. We next tested the effects of acute restraint stress on picrotoxin-induced seizure thresholds. There were no differences in the latencies to the MJ, the first stage of a picrotoxin-induced seizure (data not shown). In analysis of the latency to the second stage (atypical clonic seizure), we found a main effect of restraint stress ($F_{1,38} = 9.317$, $P < 0.01$). *Post hoc* analysis showed that there was a statistically significant decrease in the latencies of the *Scn1a*$^{RH/+}$ mutants, but not in the WT littermates (Fig. 5a). The third stage of a picrotoxin-induced seizure is the development of bilateral forelimb clonus. Again, we found a main effect of restraint stress ($F_{1,39} = 12.094$, $P < 0.01$), but this time *post hoc* analysis showed significant decreases in both the *Scn1a*$^{RH/+}$ mutants and the WT littermates (Fig. 5b). An analysis of the latency to a stage 4 picrotoxin-induced seizure, the GTCS without a tonic component, again showed a main effect of restraint stress ($F_{1,39} = 8.719$, $P < 0.01$); however, the *post hoc* analysis showed that the decrease in threshold was significant only in the *Scn1a*$^{RH/+}$ mutants (Fig. 5c). There were no differences in latencies to the stage

5 picrotoxin-induced seizure (GTCS with tonic hindlimb extension); however, it was observed that the stressed *Scn1a*$^{RH/+}$ mutants were having many more repeated stage 4 seizures prior to advancing to a stage 5 seizure (*Scn1a*$^{RH/+}$ mutants, 6.5 ± 1.5 stage 4 seizures; WT littermates, 2.8 ± 0.8 stage 4 seizures; $t_{19} = -2.05$, $P = 0.054$). While stress was sufficient to decrease seizure thresholds in both genotypes, the stress effects in the *Scn1a*$^{RH/+}$ mutants appeared to be slightly more pronounced than those seen in the WT littermates.

Scn1a$^{RH/+}$ mutants have similar HPA axis function as WT littermates

There were no differences between genotypes in basal CORT levels (Fig. 5d). In response to an acute 20-min restraint stress, there were again no genotype differences, although we did note that the *Scn1a*$^{RH/+}$ mutants had a greater variation in their CORT response (Fig. 5e). The CORT levels in the evening (1900 h) on the same day as the morning exposure to acute restraint stress in both *Scn1a*$^{RH/+}$ mutants and WT littermates were elevated as compared with normal, non-stressed 1900 h CORT levels (Fig. 5f). A two-way rANOVA showed a main effect of stress ($F_{1,20} = 9.294$, $P < 0.01$).

N12 Scn1a^{RH} mutants exhibit a shortened life span, spontaneous seizures and a reduced latency to flurothyl-induced seizures

We also characterized the *Scn1a* R1648H mutation on an N12 C57BL/6J background. Beginning at P10, *Scn1a*$^{RH/RH}$ mutants began to show slower weight gain, with weight loss and premature mortality beginning around P16 (Fig. S1a,b). There was a significant main effect of genotype when comparing pre-weaning weights ($F_{2,129} = 29.086$, $P < 0.001$), but there was also a significant interaction between genotype and age ($F_{38,2402} = 97.646$, $P < 0.001$), with only the *Scn1a*$^{RH/RH}$ mutants showing a slower growth rate beginning around P10 and a subsequent loss of weight around P16 (Fig. S1a).Homozygous *Scn1a*$^{RH/RH}$ mutants have a significantly shorter life span when compared with both *Scn1a*$^{RH/+}$ mutants (log-rank statistic: 111.555, $P < 0.001$) and WT littermates (log-rank statistic: 76.407, $P < 0.001$) (Fig. S1b) as reported previously at the N2 generation (Martin *et al.* 2010). However, the average life span of N12 heterozygous *Scn1a*$^{RH/+}$ mutants is also significantly different from WT littermates (log-rank statistic: 5.698, $P < 0.05$; Fig. S1b), a novel finding of this study.

After weaning, there were too few surviving *Scn1a*$^{RH/RH}$ mutants to include in analysis of post-weaning weights. There were no statistically significant differences in the post-weaning weights of male *Scn1a*$^{RH/+}$ mutants as compared with male WT littermates (Fig. S1c), nor were there any differences in post-weaning weights between heterozygous female mutants and WT littermates (data not shown).

Spontaneous seizures were observed in both heterozygous *Scn1a*$^{RH/+}$ mutants and homozygous *Scn1a*$^{RH/RH}$ mutants during daily weighing sessions as well as during routine mouse colony management procedures. We also asked whether the N12 *Scn1a*$^{RH/+}$ mutants would exhibit increased susceptibility to flurothyl-induced seizures as was previously observed in the N2 *Scn1a*$^{RH/+}$ mutants. Similar to the N2 mutants, there was no difference in latency to the MJ, but *Scn1a*$^{RH/+}$ mutants showed a significantly lower latency to the flurothyl-induced GTCS (*Scn1a*$^{RH/+}$, 6.5 ± 0.4 min; WT, 7.5 ± 0.2 min; $t_{27} = 2.844$, $P < 0.01$; Fig. S1d).

Discussion

Our original characterization of the *Scn1a*^{RH} mutants was performed at the N2 generation on a mixed 129X1/SvJ × C57BL/6J background. Because the genetic background is known to affect seizure and behavioral phenotypes and stress responsivity (Anisman *et al.* 2001; Brinks *et al.* 2008; Moy *et al.* 2004; Schauwecker 2002), we decided to backcross the *Scn1a* R1648H line to the C57BL/6J background for 12 generations. We have previously shown that the heterozygous N2 *Scn1a*$^{RH/+}$ mutants exhibit a normal life span, infrequent spontaneous seizures and a reduced latency to flurothyl-induced seizures (Martin *et al.* 2010). While the seizure phenotype of N12 *Scn1a*$^{RH/+}$ mutants was similar, we observed a statistically significant difference in life span when compared with WT littermates. The difference in survival of the N2 and N12 *Scn1a*$^{RH/+}$ mutants is likely due to differences in the genetic background as previously reported for *Scn1a* knockout mice (Miller *et al.* 2014; Ogiwara *et al.* 2007; Yu *et al.* 2006). Both N2 and N12 homozygous *Scn1a*$^{RH/RH}$ mutants exhibited spontaneous seizures and significant slowing in growth rate beginning at P10. Average life spans were comparable for the homozygous mutants of both generations (N2, 18.5 days; N12, 24.5 days).

It has previously been reported that mice with reduced *Scn1a* expression exhibit hyperactivity, social deficits, anxiety and impaired spatial learning and memory (Han *et al.* 2012; Ito *et al.* 2012). While many of the clinical features of DS are recapitulated in *Scn1a* knockout mice, the neuropsychiatric comorbidities and cognitive deficits that may occur in GEFS+ have not been well studied in an animal model. In this study, we have shown that *Scn1a*$^{RH/+}$ mutants also demonstrate hyperactivity, social deficits and impaired learning and memory. While *Scn1a* knockout mice show profound social deficits, the *Scn1a*$^{RH/+}$ mutants exhibited normal responses to social contact and social odor; however, deficits in preference for social novelty as well as reduced mating calls were observed.

We have previously shown that *Scn1a* is expressed in a large percentage of the parvalbumin interneurons in the hippocampus (91%) and neocortex (78%) (Dutton *et al.* 2013). The hippocampus is known to be an important region for spatial learning (Foster & Knierim 2012), and a recent study by Reichel *et al.* (2014) showed that GABAergic depletion in the dorsal hippocampus, triggered in part by the loss of parvalbumin neurons, caused hyperactivity and interfered with the acquisition of spatial memory. Furthermore, kindling of the prefrontal cortex resulted in both PPI deficit and hyperactivity (Ma & Leung 2010). Thus, the loss of inhibitory signaling in both the hippocampus and neocortex could underlie the deficits in spatial memory, the hyperactivity and the reduction in PPI observed in the *Scn1a*$^{RH/+}$ mutants. The reduction

in PPI of the acoustic startle response, a process that involves a pre-attentive gating mechanism of incoming sensory stimuli, has not been previously described in *Scn1a* mutants and further extends the spectrum of behavioral alterations associated with *Scn1a* dysfunction. Intriguingly, it was recently reported that WAG-Rij rats, a model of genetic absence epilepsy, also have deficits in PPI which were reversed by lamotrigine (Celikyurt *et al*. 2012), an antiepileptic drug that works by blocking VGSCs and increasing GABAergic neurotransmission (Cunningham & Jones 2000). In further support of the hypothesis that reduction in *Scn1a* function in interneurons underlies these behavioral phenotypes, Reichel *et al*. (2014) showed that the loss of interneurons in the medial prefrontal cortex led to deficits in sensorimotor gating, and Shamir *et al*. (2012) showed that alterations in parvalbumin interneurons were correlated with hyperactivity, reductions in PPI and deficits in cued fear conditioning. These recent findings suggest that the dysfunction of *Scn1a* in parvalbumin interneurons could be driving the sensorimotor and learning deficits as well as the hyperactivity observed in the *Scn1a*$^{RH/+}$ mutants. To date, the only form of human epilepsy linked to deficits in PPI is temporal lobe epilepsy with psychosis (Braff *et al*. 2001), but given the increasing amount of evidence linking PPI and other behaviors to decreases in inhibitory signaling, it may be worthwhile to examine patients with *SCN1A* mutations for PPI deficits.

After observing that the *Scn1a*$^{RH/+}$ mutants froze less than WT littermates when exposed to predator odor, we wondered if the mutants might have an altered ability to assess risk. Our findings in the visual cliff task would appear to support this idea. While it is well established that some behavioral and neuropsychiatric abnormalities can occur in patients with epilepsy, risk-taking behavior in this population has been poorly studied. Alfstad *et al.* (2011) reported that risk-taking behaviors were more prevalent in young boys with epilepsy than in controls. Risk-taking behavior in humans has been associated with altered patterns of prefrontal cortex activity (Studer *et al*. 2013), and as mentioned previously, *Scn1a* is expressed in 78% of the parvalbumin neurons of the neocortex (Dutton *et al*. 2013). While it is possible that these observed behaviors may be related to the hyperactive phenotype, this intriguing potential new phenotype in the *Scn1a*$^{RH/+}$ mutants may highlight the importance of *Scn1a* expression in the prefrontal cortex and opens up new avenues of investigation into comorbidities associated with *Scn1a* dysfunction.

We recently showed that a mutation in another VGSC, *Scn8a*, can alter the seizure response to a stressor (Sawyer *et al.* 2014). In this study, we found that acute restraint stress did reduce thresholds to picrotoxin-induced seizures, and although the direction of change was the same in both WT littermates and *Scn1a*$^{RH/+}$ mutants, the magnitude of the change was larger in the *Scn1a*$^{RH/+}$ mutants. Furthermore, *Scn1a* dysfunction does not appear to affect normal functioning of the HPA axis, one of the primary physiological stress response systems. While these results differ from the ones found with the *Scn8a* mutants, the differences shed light on possible pathophysiological mechanisms. *Scn8a* mutants have deficits in excitatory signaling, spontaneous absence seizures and an increased resistance to chemiconvulsant-induced seizures (Martin *et al*. 2007; Papale *et al*. 2009). The *Scn8a* mutants also showed measures of increased anxiety which could have triggered long-lasting changes in HPA axis activity as well as altering the seizure response to stress (Sawyer *et al*. 2014). The *Scn1a*$^{RH/+}$ mutants did not show any differences in the measures of anxiety tested in this study, and perhaps for this reason the effect of stress on the response to picrotoxin-induced seizures is similar between *Scn1a*$^{RH/+}$ mutants and WT littermates. While we found that unstressed *Scn1a*$^{RH/+}$ mutants had a shorter latency to flurothyl-induced GTCS, the unstressed *Scn1a*$^{RH/+}$ mutants did not exhibit a similar shorter latency to picrotoxin-induced GTCS. This difference is likely because of the different pharmacological effects of these chemiconvulsants on the central nervous system; while picrotoxin is a noncompetitive $GABA_A$ receptor antagonist, the mechanism for the convulsive activity of flurothyl is less clear and has been shown to have multiple targets: directly affecting VGSCs, inhibiting GABA and activating the cholinergic system (Velisek 2006). Another interesting finding of this study is that chronic restraint stress only increased spontaneous seizure activity in the *Scn1a*$^{RH/+}$ mutants that were already exhibiting spontaneous seizures, suggesting that while stress can precipitate spontaneous seizures in an already seizing animal, it may not be sufficient to cause seizures in a mutant that does not have a history of spontaneous seizures. A recent study by MacKenzie and Maguire (2015) showed that chronic stress can shift the GABA reversal potential in the hippocampus, thereby increasing the intrinsic excitability of hippocampal pyramidal neurons. We speculate that *Scn1a*$^{RH/+}$ mutants that were already seizing prior to the chronic stressor potentially had more of a reduction in interneuron signaling and thus were likely to be more affected by a stress-induced increase in excitability following chronic stress.

In summary, we have shown that the *Scn1a*$^{RH/+}$ phenotype is more severe after backcrossing to the C57BL/6J background for 12 generations, providing support for the hypothesis that other modifier genes could contribute to the clinical heterogeneity seen in GEFS+ families. We also verified autistic-like traits such as hyperactivity and social deficits as well as deficits in spatial memory that have previously been linked with *SCN1A* dysfunction. However, this study extends the *Scn1a* phenotype to include deficits in cued fear conditioning, PPI and risk assessment which provides additional insight into the pathophysiological mechanisms underlying VGSC dysfunction. Finally, we have shown that stress can worsen seizure outcome in *Scn1a*$^{RH/+}$ mutants, but in a manner similar to the WT littermates, and the *Scn1a* mutation does not affect normal HPA axis function.

References

Alfstad, K.A., Clench-Aas, J., Van Roy, B., Mowinckel, P., Gjerstad, L. & Lossius, M.I. (2011) Gender differences in risk-taking behaviour in youth with epilepsy: a Norwegian population-based study. *Acta Neurol Scand Suppl*, **191**, 12–17.

Anisman, H., Hayley, S., Kelly, O., Borowski, T. & Merali, Z. (2001) Psychogenic, neurogenic, and systemic stressor effects on plasma corticosterone and behavior: mouse strain-dependent outcomes. *Behav Neurosci* **115**, 443–454.

Antunes, M. & Biala, G. (2012) The novel object recognition memory: neurobiology, test procedure, and its modifications. *Cogn Process* **13**, 93–110.

Baulac, S., Gourfinkel-An, I., Couarch, P., Depienne, C., Kaminska, A., Dulac, O., Baulac, M., LeGuern, E. & Nabbout, R. (2008) A novel locus for generalized epilepsy with febrile seizures plus in French families. *Arch Neurol* **65**, 943–951.

Braff, D.L., Geyer, M.A. & Swerdlow, N.R. (2001) Human studies of prepulse inhibition of startle: normal subjects, patient groups, and pharmacological studies. *Psychopharmacology (Berl)* **156**, 234–258.

Brinks, V., de Kloet, E.R. & Oitzl, M.S. (2008) Strain specific fear behaviour and glucocorticoid response to aversive events: modelling PTSD in mice. *Prog Brain Res* **167**, 257–261.

Celikyurt, I.K., Ulak, G., Mutlu, O., Akar, F.Y., Erden, F. & Komsuoglu, S.S. (2012) Lamotrigine effects sensorimotor gating in WAG/Rij rats. *J Neurosci Rural Pract* **3**, 126–130.

Ceulemans, B., Boel, M., Claes, L., Dom, L., Willekens, H., Thiry, P. & Lagae, L. (2004) Severe myoclonic epilepsy in infancy: toward an optimal treatment. *J Child Neurol* **19**, 516–521.

Chao, H.T., Chen, H., Samaco, R.C., Xue, M., Chahrour, M., Yoo, J., Neul, J.L., Gong, S., Lu, H.C., Heintz, N., Ekker, M., Rubenstein, J.L., Noebels, J.L., Rosenmund, C. & Zoghbi, H.Y. (2010) Dysfunction in GABA signalling mediates autism-like stereotypies and Rett syndrome phenotypes. *Nature* **468**, 263–269.

Cheah, C.S., Yu, F.H., Westenbroek, R.E., Kalume, F.K., Oakley, J.C., Potter, G.B., Rubenstein, J.L. & Catterall, W.A. (2012) Specific deletion of NaV1.1 sodium channels in inhibitory interneurons causes seizures and premature death in a mouse model of Dravet syndrome. *Proc Natl Acad Sci U S A* **109**, 14646–14651.

Claes, L., Del-Favero, J., Ceulemans, B., Lagae, L., Van Broeckhoven, C. & De Jonghe, P. (2001) De novo mutations in the sodium-channel gene SCN1A cause severe myoclonic epilepsy of infancy. *Am J Hum Genet* **68**, 1327–1332.

Cunningham, M.O. & Jones, R.S. (2000) The anticonvulsant, lamotrigine decreases spontaneous glutamate release but increases spontaneous GABA release in the rat entorhinal cortex in vitro. *Neuropharmacology* **39**, 2139–2146.

Dere, E., Huston, J.P. & De Souza Silva, M.A. (2005) Integrated memory for objects, places, and temporal order: evidence for episodic-like memory in mice. *Neurobiol Learn Mem* **84**, 214–221.

Douglas, R.M., Alam, N.M., Silver, B.D., McGill, T.J., Tschetter, W.W. & Prusky, G.T. (2005) Independent visual threshold measurements in the two eyes of freely moving rats and mice using a virtual-reality optokinetic system. *Vis Neurosci* **22**, 677–684.

Dutton, S.B., Sawyer, N.T., Kalume, F., Jumbo-Lucioni, P., Borges, K., Catterall, W.A. & Escayg, A. (2011) Protective effect of the ketogenic diet in Scn1a mutant mice. *Epilepsia* **52**, 2050–2056.

Dutton, S.B., Makinson, C.D., Papale, L.A., Shankar, A., Balakrishnan, B., Nakazawa, K. & Escayg, A. (2013) Preferential inactivation of Scn1a in parvalbumin interneurons increases seizure susceptibility. *Neurobiol Dis* **49C**, 211–220.

Escayg, A., MacDonald, B.T., Meisler, M.H., Baulac, S., Huberfeld, G., An-Gourfinkel, I., Brice, A., LeGuern, E., Moulard, B., Chaigne, D., Buresi, C. & Malafosse, A. (2000) Mutations of SCN1A, encoding a neuronal sodium channel, in two families with GEFS+ 2. *Nat Genet* **24**, 343–345.

Foster, D.J. & Knierim, J.J. (2012) Sequence learning and the role of the hippocampus in rodent navigation. *Curr Opin Neurobiol* **22**, 294–300.

Fujiwara, T. (2006) Clinical spectrum of mutations in SCN1A gene: severe myoclonic epilepsy in infancy and related epilepsies. *Epilepsy Res* **70** Suppl. 1, S223–S230.

Grant, A.C. & Vazquez, B. (2005) A case of extended spectrum GEFS+. *Epilepsia* **46** Suppl. 10, 39–40.

Han, S., Tai, C., Westenbroek, R.E., Yu, F.H., Cheah, C.S., Potter, G.B., Rubenstein, J.L., Scheuer, T., de la Iglesia, H.O. & Catterall, W.A. (2012) Autistic-like behaviour in Scn1a+/- mice and rescue by enhanced GABA-mediated neurotransmission. *Nature* **489**, 385–390.

Hancock, G.R. & Klockars, A.J. (1996) The quest for alpha: developments in multiple comparison procedures in the quarter century since Games (1971). *Rev Educ Res* **66**, 269–306.

Ito, S., Ogiwara, I., Yamada, K., Miyamoto, H., Hensch, T.K., Osawa, M. & Yamakawa, K. (2012) Mouse with Na(v)1.1 haploinsufficiency, a model for Dravet syndrome, exhibits lowered sociability and learning impairment. *Neurobiol Dis* **49C**, 29–40.

Ma, J. & Leung, L.S. (2010) Kindled seizure in the prefrontal cortex activated behavioral hyperactivity and increase in accumbens gamma oscillations through the hippocampus. *Behav Brain Res* **206**, 68–77.

MacKenzie, G. & Maguire, J. (2015) Chronic stress shifts the GABA reversal potential in the hippocampus and increases seizure susceptibility. *Epilepsy Res* **109**, 13–27.

Mahoney, K., Moore, S.J., Buckley, D., Alam, M., Parfrey, P., Penney, S., Merner, N., Hodgkinson, K. & Young, T.L. (2009) Variable neurologic phenotype in a GEFS+ family with a novel mutation in SCN1A. *Seizure* **18**, 492–497.

Martin, M.S., Tang, B., Papale, L.A., Yu, F.H., Catterall, W.A. & Escayg, A. (2007) The voltage-gated sodium channel Scn8a is a genetic modifier of severe myoclonic epilepsy of infancy. *Hum Mol Genet* **16**, 2892–2899.

Martin, M.S., Dutt, K., Papale, L.A., Dube, C.M., Dutton, S.B., de Haan, G., Shankar, A., Tufik, S., Meisler, M.H., Baram, T.Z., Goldin, A.L. & Escayg, A. (2010) Altered function of the SCN1A voltage-gated sodium channel leads to gamma-aminobutyric acid-ergic (GABAergic) interneuron abnormalities. *J Biol Chem* **285**, 9823–9834.

Miller, A.R., Hawkins, N.A., McCollom, C.E. & Kearney, J.A. (2014) Mapping genetic modifiers of survival in a mouse model of Dravet syndrome. *Genes Brain Behav* **13**, 163–172.

Moy, S.S., Nadler, J.J., Perez, A., Barbaro, R.P., Johns, J.M., Magnuson, T.R., Piven, J. & Crawley, J.N. (2004) Sociability and preference for social novelty in five inbred strains: an approach to assess autistic-like behavior in mice. *Genes Brain Behav* **3**, 287–302.

Mulley, J.C., Scheffer, I.E., Petrou, S., Dibbens, L.M., Berkovic, S.F. & Harkin, L.A. (2005) SCN1A mutations and epilepsy. *Hum Mutat* **25**, 535–542.

Ogiwara, I., Miyamoto, H., Morita, N., Atapour, N., Mazaki, E., Inoue, I., Takeuchi, T., Itohara, S., Yanagawa, Y., Obata, K., Furuichi, T., Hensch, T.K. & Yamakawa, K. (2007) Na(v)1.1 localizes to axons of parvalbumin-positive inhibitory interneurons: a circuit basis for epileptic seizures in mice carrying an Scn1a gene mutation. *J Neurosci* **27**, 5903–5914.

O'Roak, B.J., Vives, L., Girirajan, S. *et al.* (2012) Sporadic autism exomes reveal a highly interconnected protein network of de novo mutations. *Nature* **485**, 246–250.

Osaka, H., Ogiwara, I., Mazaki, E., Okamura, N., Yamashita, S., Iai, M., Yamada, M., Kurosawa, K., Iwamoto, H., Yasui-Furukori, N., Kaneko, S., Fujiwara, T., Inoue, Y. & Yamakawa, K. (2007) Patients with a sodium channel alpha 1 gene mutation show wide phenotypic variation. *Epilepsy Res* **75**, 46–51.

Paluszkiewicz, S.M., Martin, B.S. & Huntsman, M.M. (2011) Fragile X syndrome: the GABAergic system and circuit dysfunction. *Dev Neurosci* **33**, 349–364.

Papale, L.A., Beyer, B., Jones, J.M., Sharkey, L.M., Tufik, S., Epstein, M., Letts, V.A., Meisler, M.H., Frankel, W.N. & Escayg, A. (2009) Heterozygous mutations of the voltage-gated sodium channel SCN8A are associated with spike-wave discharges and absence epilepsy in mice. *Hum Mol Genet* **18**, 1633–1641.

Papale, L.A., Paul, K.N., Sawyer, N.T., Manns, J.R., Tufik, S. & Escayg, A. (2010) Dysfunction of the Scn8a voltage-gated sodium channel alters sleep architecture, reduces diurnal corticosterone levels, and enhances spatial memory. *J Biol Chem* **285**, 16553–16561.

Papale, L.A., Makinson, C.D., Christopher Ehlen, J., Tufik, S., Decker, M.J., Paul, K.N. & Escayg, A. (2013) Altered sleep regulation in a mouse model of SCN1A-derived genetic epilepsy with febrile seizures plus (GEFS+). *Epilepsia* **54**, 625–634.

Purcell, R.H., Papale, L.A., Makinson, C.D., Sawyer, N.T., Schroeder, J.P., Escayg, A. & Weinshenker, D. (2013) Effects of an

epilepsy-causing mutation in the SCN1A sodium channel gene on cocaine-induced seizure susceptibility in mice. *Psychopharmacology (Berl)* **228**, 263–270.
Ragsdale, D.S. (2008) How do mutant Nav1.1 sodium channels cause epilepsy? *Brain Res Rev* **58**, 149–159.
Reichel, J.M., Nissel, S., Rogel-Salazar, G., Mederer, A., Kafer, K., Bedenk, B.T., Martens, H., Anders, R., Grosche, J., Michalski, D., Hartig, W. & Wotjak, C.T. (2014) Distinct behavioral consequences of short-term and prolonged GABAergic depletion in prefrontal cortex and dorsal hippocampus. *Front Behav Neurosci* **8**, 452.
Sawyer, N.T., Papale, L.A., Eliason, J., Neigh, G.N. & Escayg, A. (2014) Scn8a voltage-gated sodium channel mutation alters seizure and anxiety responses to acute stress. *Psychoneuroendocrinology* **39**, 225–236.
Schauwecker, P.E. (2002) Complications associated with genetic background effects in models of experimental epilepsy. *Prog Brain Res* **135**, 139–148.
Scheffer, I.E. & Berkovic, S.F. (1997) Generalized epilepsy with febrile seizures plus. A genetic disorder with heterogeneous clinical phenotypes. *Brain* **120**, 479–490.
Shamir, A., Kwon, O.B., Karavanova, I., Vullhorst, D., Leiva-Salcedo, E., Janssen, M.J. & Buonanno, A. (2012) The importance of the NRG-1/ErbB4 pathway for synaptic plasticity and behaviors associated with psychiatric disorders. *J Neurosci* **32**, 2988–2997.
Studer, B., Pedroni, A. & Rieskamp, J. (2013) Predicting risk-taking behavior from prefrontal resting-state activity and personality. *PLoS One* **8**, e76861.
Tang, B., Dutt, K., Papale, L., Rusconi, R., Shankar, A., Hunter, J., Tufik, S., Yu, F.H., Catterall, W.A., Mantegazza, M., Goldin, A.L. & Escayg, A. (2009) A BAC transgenic mouse model reveals neuron subtype-specific effects of a generalized epilepsy with febrile seizures plus (GEFS+) mutation. *Neurobiol Dis* **35**, 91–102.
Velisek, L. (2006) Models of chemically-induced acute seizures. In Pitkanen, A., Schwartzkroin, P.A. & Moshe, S.L. (eds), *Models of Seizures and Epilepsy*. Elsevier, Amsterdam, pp. 127–152.
Veliskova, J. (2006) Behavioral characterization of seizures in rats. In Pitkanen, A., Schwartzkroin, P.A. & Moshe, S.L. (eds), *Models of Seizures and Epilepsy*. Elsevier, Amsterdam, pp. 601–611.
Ware, W.B., Ferron, J.M. & Miller, B.M. (2012) *Introductory Statistics: A Conceptual Approach Using R*. Routledge, New York, NY.
Weiss, L.A., Escayg, A., Kearney, J.A., Trudeau, M., MacDonald, B.T., Mori, M., Reichert, J., Buxbaum, J.D. & Meisler, M.H. (2003) Sodium channels SCN1A, SCN2A and SCN3A in familial autism. *Mol Psychiatry* **8**, 186–194.
Wolff, M., Casse-Perrot, C. & Dravet, C. (2006) Severe myoclonic epilepsy of infants (Dravet syndrome): natural history and neuropsychological findings. *Epilepsia* **47** Suppl. 2, 45–48.
Yu, F.H., Mantegazza, M., Westenbroek, R.E., Robbins, C.A., Kalume, F., Burton, K.A., Spain, W.J., McKnight, G.S., Scheuer, T. & Catterall, W.A. (2006) Reduced sodium current in GABAergic interneurons in a mouse model of severe myoclonic epilepsy in infancy. *Nat Neurosci* **9**, 1142–1149.

Acknowledgments

This study was supported by grants from the NIH (R01NS072221 and R21NS084229 to A.E. and 1F31NS073237-01 to N.T.S.) and an ARCS Fellowship (N.T.S.). This material is also based upon work supported by the University of West Georgia's Internal Development Grant Fund (Grant ID 13-1014023 to A.W.H.). We would like to thank Dr David Weinshenker and Dr Jason Schroeder of the Emory University Behavioral Core for performing the fear conditioning experiment. We would like to thank Dr Xiao-Jiang Li and Dr Shi-Hua Li for providing access to their equipment for PPI analysis. We would also like to thank Dr Machelle Pardue and Megan Prunty for performing the visual function test, and Dr Robert Liu and Katy Shepard for assistance with recording the mating calls. The authors declare no conflicts of interest in relation to the work described in this manuscript.

Supporting Information

Additional supporting information may be found in the online version of this article at the publisher's web-site:

Video S1 This video file shows a *Scn1a*$^{RH/+}$ mutant having a GTCS with simultaneous EEG recording. At the beginning of the clip, normal EEG activity is being recorded. The beginning of the GTCS occurs 00:23 seconds into the recording and is accompanied by epileptiform EEG activity (sharp waves increasing in frequency and achieving amplitudes at least two times the size of background waves). The EEG is accompanied by characteristic seizure behavior such as forelimb clonus with preserved righting reflex (beginning at 00:37 seconds) followed by the loss of the righting reflex (00:41 seconds), continued clonus with some tonus and culminating in wild running behavior (01:07 min). After the seizure is over (01:12 in), EEG signal is significantly reduced, characteristic of a post-seizure refractory period.

Figure S1 Characterization of the N12 C57BL/6J *Scn1a* R1448H mutant line. (a) The pre-weaning weight gain of *Scn1a*$^{RH/+}$ mutants ($n = 76$) and WT littermates ($n = 31$) are indistinguishable; however, *Scn1a*$^{RH/RH}$ mutants ($n = 37$) show a significant reduction in weight gain around P10, and a reduction in body weight beginning around P16. $^*P < 0.05$ vs. WT and *Scn1a*$^{RH/+}$. (b) Both *Scn1a*$^{RH/+}$ mutants ($n = 77$) and *Scn1a*$^{RH/RH}$ mutants ($n = 38$) exhibited a statistically significant reduction in life span compared with WT littermates ($n = 31$). (c) Post-weaning weights of male *Scn1a*$^{RH/+}$ mutants ($n = 34$) are not significantly different from the post-weaning weights of male WT littermates ($n = 17$). (d) There is no difference in latency to an MJ between *Scn1a*$^{RH/+}$ mutants ($n = 14$) and WT littermates ($n = 15$); however, *Scn1a*$^{RH/+}$ mutants show a signification reduction in latency to a GTCS. $^*P < 0.05$ vs. WT. Error bars represent SEM.